Supporting Information

Building Z-scheme Heterojunction with Keggin-type Heteropolymers Modified Two-dimensional g-C_3N_4 for Significantly Photocatalytic Performance

Huimin Han[a], Jinyuan Liu[b,*], Bin Wang[b], Shumin Zhu[b], Shihao Jia[a], Qi Tang[a], Yingjie Hua[a,*], Huaming Li[b], Chongtai Wang[a], Hui Xu [b,*]

[a] *School of Chemistry and Chemical Engineering of Hainan Normal University, Key Laboratory of Electrochemical Energy Storage and Energy Conversion of Hainan Province, Key Laboratory of Electrochemical Energy Storage and Light Energy Conversion Materials of Haikou City, Haikou, 571158, P.R. China.*

[b] *Institute for Energy Research, Jiangsu University, Zhenjiang 212013, Jiangsu, P. R. China*

***Corresponding author:** jyliu@ujs.edu.cn; 521000hua282@sina.com; xh@ujs.edu.cn*

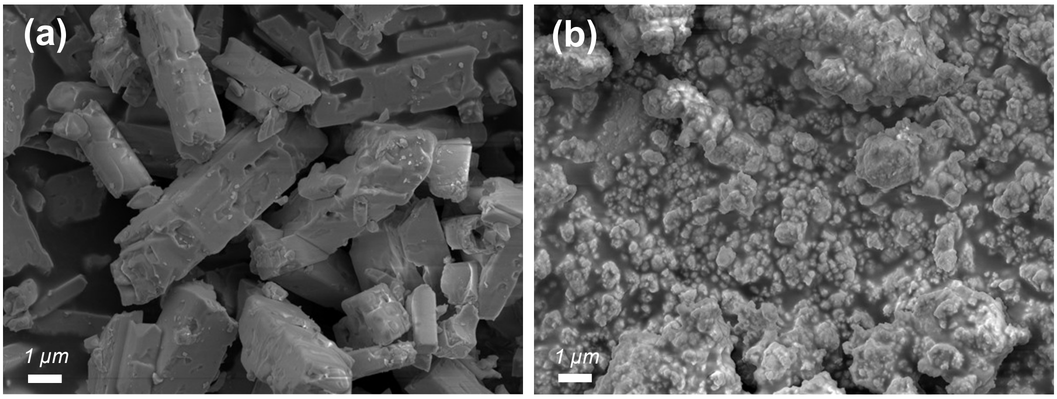

Fig. S1. SEM images of (a) $Cs_5PW_{11}Co$ and (b) $Cs_4PW_{11}Fe$

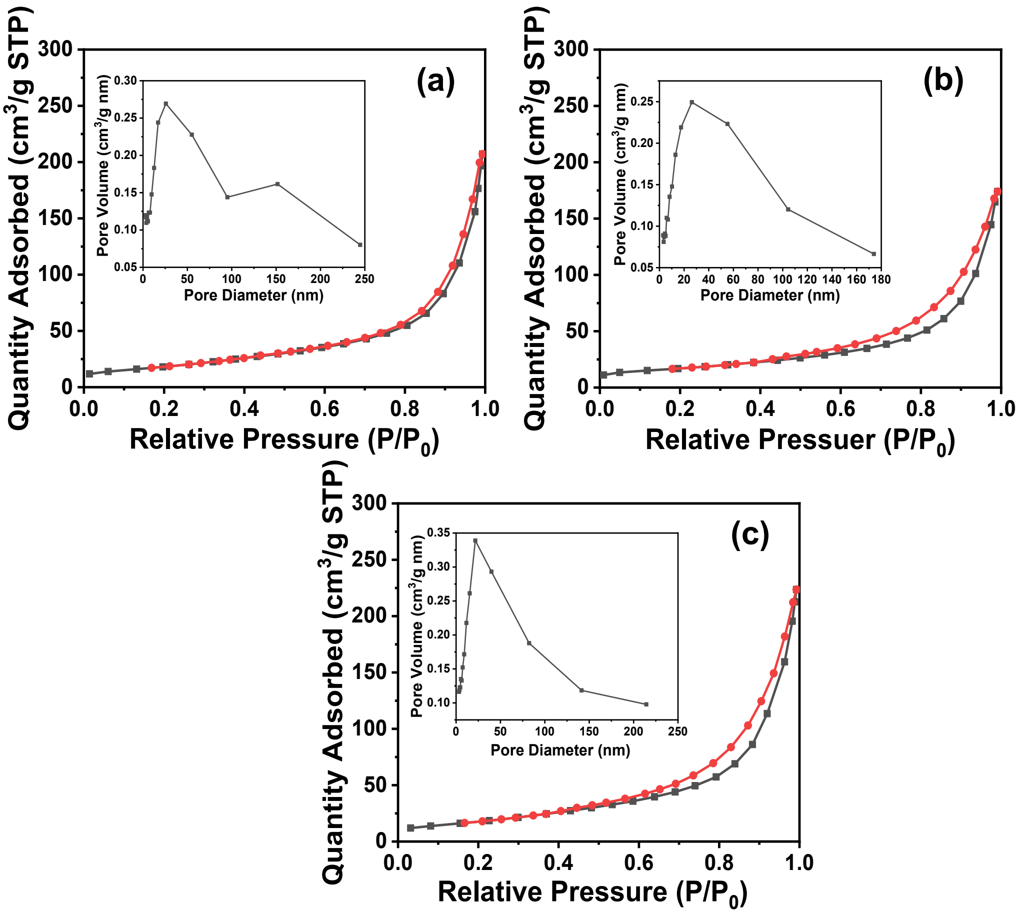

Fig. S2. N_2 adsorption-desorption isotherms and the corresponding pore size distribution curves of (a) g-C_3N_4, (b) 3 wt.% $Cs_5PW_{11}Co$/g-C_3N_4, (c) 3 wt.% $Cs_4PW_{11}Fe$/g-C_3N_4

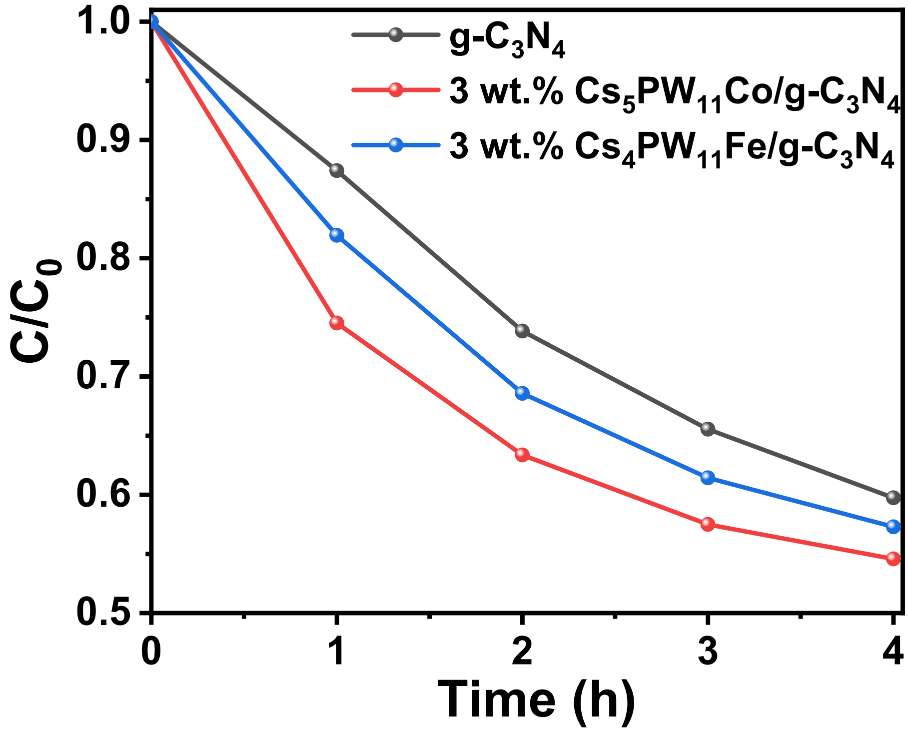

Fig. S3. Trapping experiment of active species during the photocatalytic degradation of BPA over 3 wt.% $Cs_5PW_{11}Co/g\text{-}C_3N_4$ and 3 wt.% $Cs_4PW_{11}Fe/g\text{-}C_3N_4$ under visible light irradiation

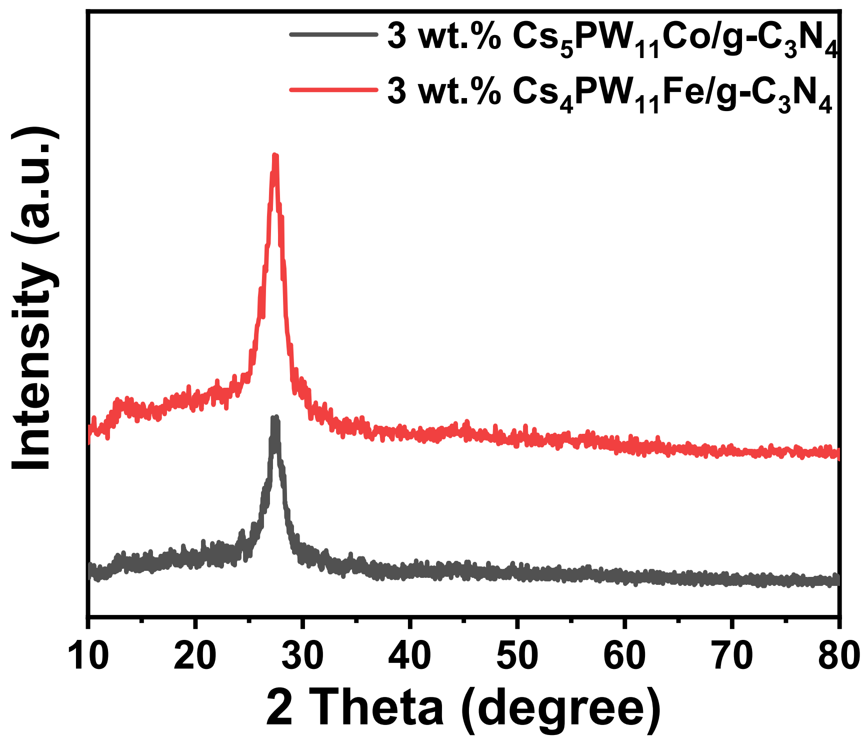

Fig. S4. XRD patterns of the 3 wt.% $Cs_5PW_{11}Co/g\text{-}C_3N_4$ and 3 wt.% $Cs_4PW_{11}Fe/g\text{-}C_3N_4$ materials after the cycling photocatalytic experiments.

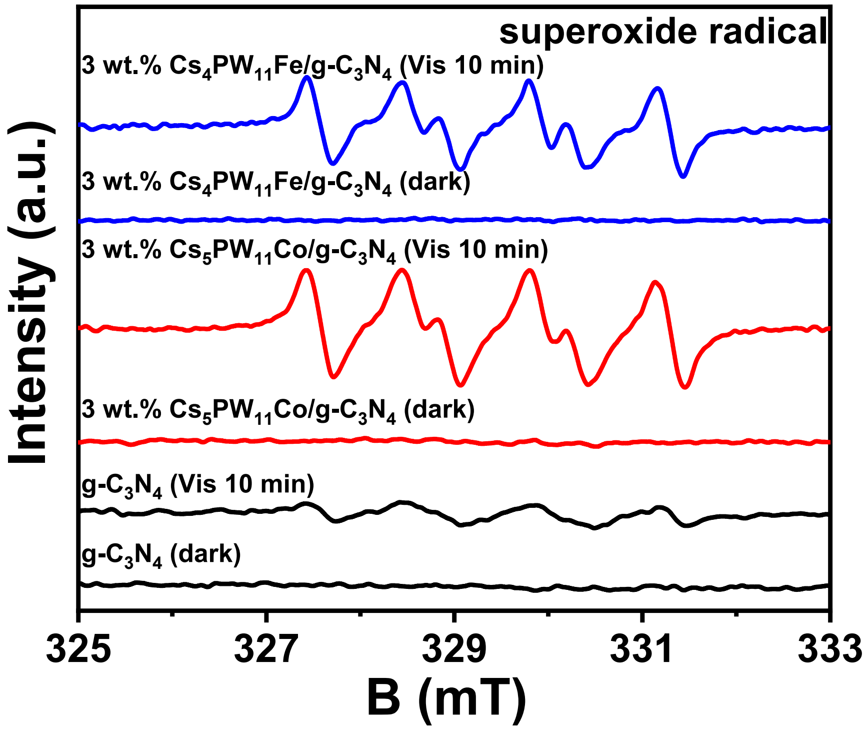

Fig. S5. ESR spectrum of 3 wt.% $Cs_xPW_{11}M/g-C_3N_4$ (M=Co, Fe) and 2D $g-C_3N_4$ radical trapped by DMPO: $\cdot O_2^-$ radical species under visible light irradiation and in dark

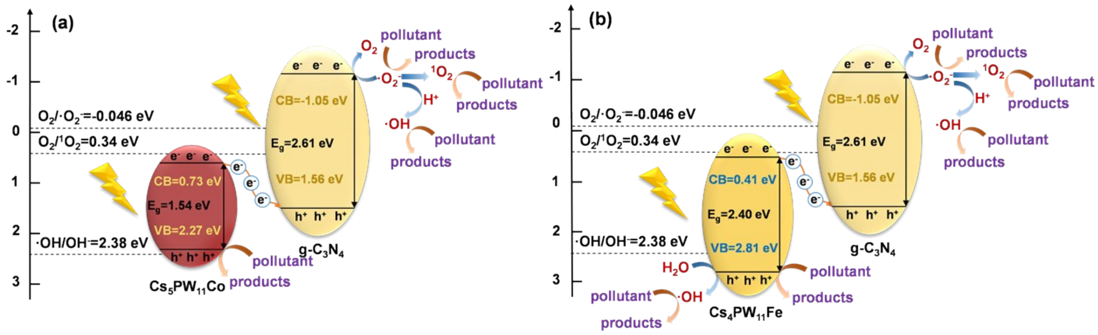

Fig. S6. The possible photocatalytic mechanism in (a) $Cs_5PW_{11}Co/g-C_3N_4$ system and (b) $Cs_4PW_{11}Fe/g-C_3N_4$ system.

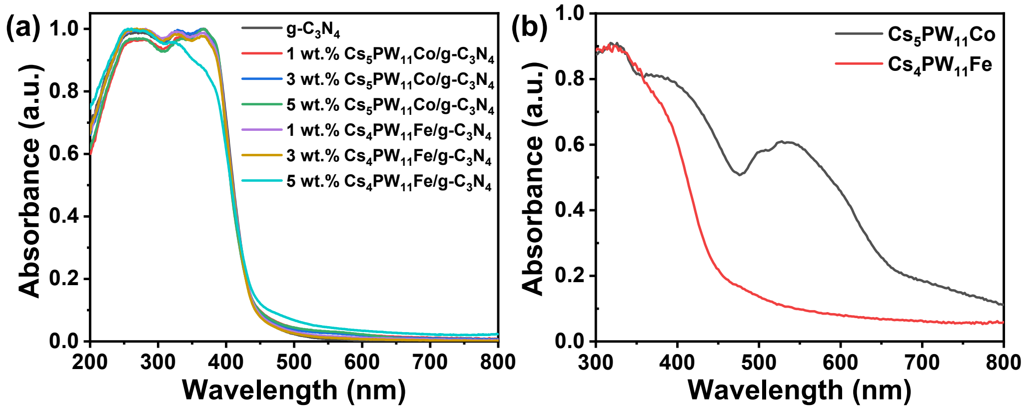

Fig. S7. UV-vis spectra (a) g-C_3N_4 and $Cs_xPW_{11}M$/g-C_3N_4 at different contents, (b) $Cs_xPW_{11}M$ (M=Co, Fe).

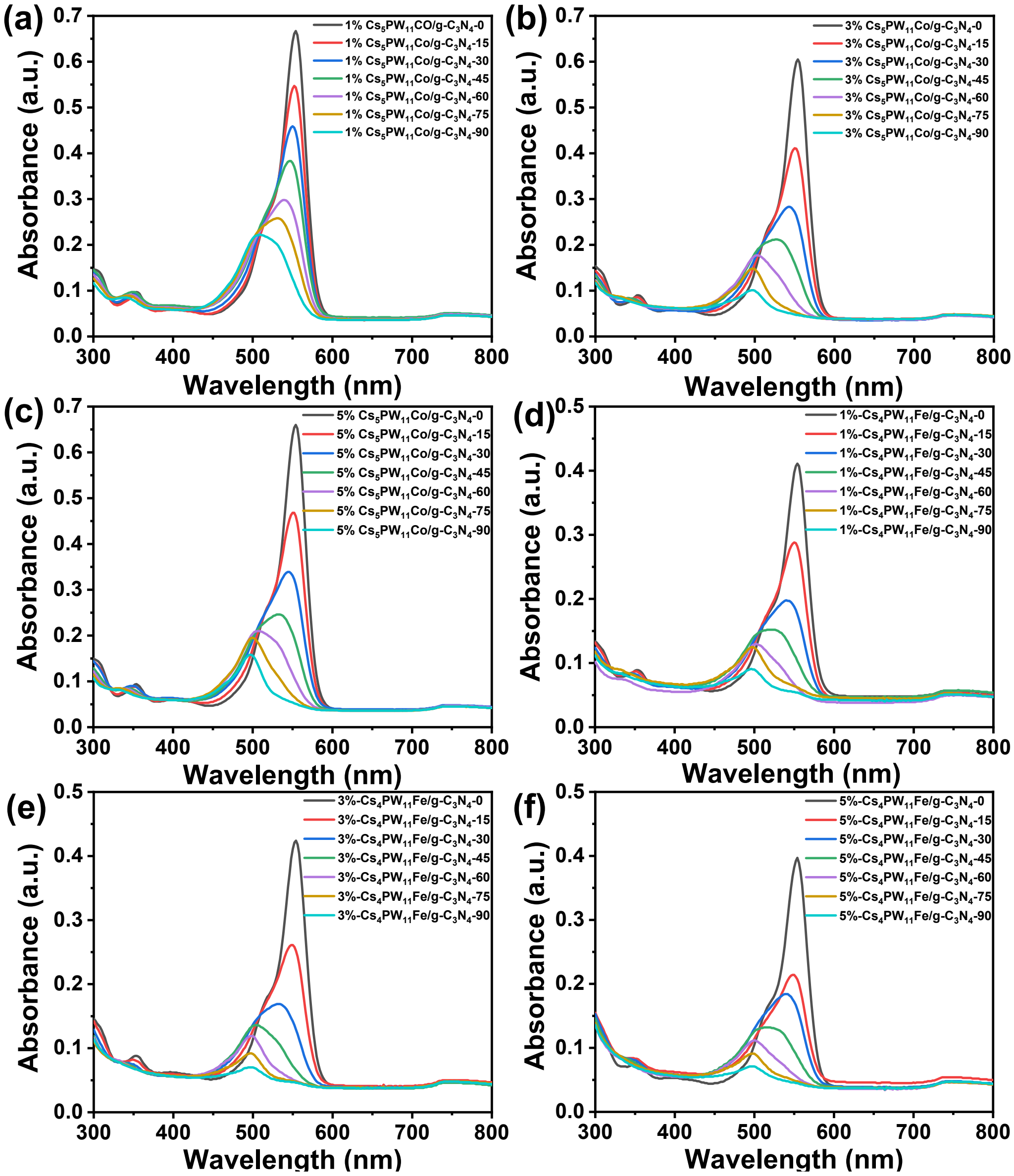

Fig. S8. (a-f) absorption spectral of RhB by $Cs_xPW_{11}M/g\text{-}C_3N_4$.

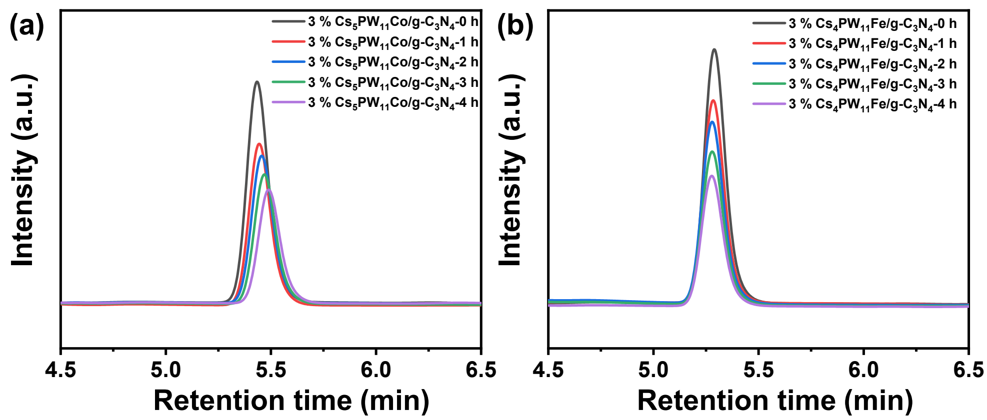

Fig. S9. (a, b) HPLC spectrums of BPA solution degraded by 3 wt.% $Cs_xPW_{11}M/g\text{-}C_3N_4$.

Table S1. Absolute electronegativity of each constituent element

Atom	Cs	P	W	O	Fe	Co
X (eV)	2.18	5.62	4.40	7.54	4.06	4.30

Table S2. Comparison of RhB degradation among different catalysts.

Photocatalysts	**Initial concentration**	**Light source and irradiation time**	**Removal efficiency**	**Ref.**
$Bi_2WO_6/ZnWO_4$	10 mg/L	500 W Xe lamp 4 h	89%	S1
NiS/ZnO	2.01×10^{-5}mol/L	8W UV-light 2h	93%	S2
CeO_2/CdS quantum dots	10 mg/L	300 W Xe lamp 3 h	96.16%	S3
g-C_3N_4/H-TiO_2	10 mg/L	300 W Xe lamp 2 h	65%	S4
Bi_3O_4Cl/Bi_5O_7I	17 ppm	300 W Xe lamp 90 min	97%	S5
$AgIO_3/WO_3$	2×10^{-5}mol/L	300 W Xe lamp 140 min	100%	S6
BiOCl/H^+ $TiNbO_5^-$	10 mg/L	250 W Xe lamp 90 min	99%	S7
g-C_3N_4/CQDs/CC	5 mg/L	250 W Xe lamp 90 min	92%	S8

Table S3. Comparison of RhB degradation among g-C_3N_4 based materials.

Photocatalysts	**Initial**	**Light source and**	**Removal**	**Ref.**

	concentration	irradiation time	efficiency	
GQDs/mpg-C_3N_4	10 mg/L	300 W Xe lamp 2 h	97%	S9
Ultrathin g-C_3N_4	30 ppm	300 W Xe lamp 90 min	100%	S10
Thin porous amino-rich g-C_3N_4	10 mg/L	500 W Xe lamp 1 h	99%	S11
g-C_3N_4/H-TiO_2	10 mg/L	300 W Xe lamp 2 h	65%	S12
S-g-C_3N_4	10 mg/L	500W Xe lamp 2 h	90%	S13
g-C_3N_4/CNTs	10 mg/L	300 W Xe lamp 1 h	98.1%	S14
Ag/AgCl-CN	5 mg/L	300 W Xe lamp 120 min	98.5%	S15
P-Cl/g-C_3N_4	10 mg/L	CEL-LED 100lamp 70 W 120 min	99.62%	S16

References

S1 Y. Rao, H. Liu, B. Zhong, Z. Li, In-situ construction of Bi_2WO_6/$ZnWO_4$ heterojunctions with enhanced photocatalytic performance toward RhB degradation. *Mater. Lett.*, 2022, **312**, 131707.

S2 S.K.Pandey, P. K. Mishra, D. Tiwary, Enhanced photocatalytic performance of NiS/ZnO nanocomposite for the remediation of PNP and RhB dye. *J. Environ. Chem. Eng.*, 2022, **10**, 107459.

S3 H. Pei, Q. Jia, R. Guo, T. Zhang, N. Liu, Z. Mo, Flower-like CeO_2/CdS quantum dots heterojunction nanocomposites with high photocatalytic activity for RhB degradation. *Colloids Surf., A*, 2022, **648**, 129256.

S4 B. Yu, C. Miao, D. Wang, H. Li, D. Sun, W. Jiang, C. Liu, G. Che, Preparation of visible light responsive g-C_3N_4/H-TiO_2 Z-scheme heterojunction with enhanced photocatalytic activity for RhB degradation. *J. Mater. Sci.: Mater. Electron.*, 2022, **33,** 17587-17598.

S5 S. T. U. Din, H. Lee, W. Yang, Z-Scheme Heterojunction of 3-Dimensional Hierarchical

Bi_3O_4Cl/Bi_5O_7I for a Significant Enhancement in the Photocatalytic Degradation of Organic Pollutants (RhB and BPA). *Nanomaterials*, 2022, **12**, 767.

S6 Q. Cao, Y. Zheng, X Song. Enhanced visible-light-driven photocatalytic degradation of RhB by $AgIO_3/WO_3$ composites. *J. Taiwan Inst. Chem. Eng*, 2017, **70**, 359-365.

S7 C. Liu, X. Gao, C. Zhangai, T. Cheng, Y. Wang, Layered $BiOCl/H^+$ $TiNbO_5^-$ heterojunctions for boosting visible-light-driven photocatalytic RhB degradation. *Sustainable Energy Fuels*, 2021, **5**, 4680-4689.

S8 B Zhu, X Li, Y Wang, N. Liu, Y. Tian, Visible-light-driven photocatalytic degradation of RhB by carbon-quantum-dot-modified g-C_3N_4 on carbon cloth. *CrystEngComm*, 2021, **23**, 4782-4790.

S9 J. Liu, H. Xu, Y. Xu, Y. Song, Graphene quantum dots modified mesoporous graphite carbon nitride with significant enhancement of photocatalytic activity. *Appl. Catal. B*, 2017, **207**, 429-437.

S10 S. Gao, X. Wang, C. Song, S. Zhou, F. Yang and Y. Kong, Engineering carbon-defects on ultrathin g-C_3N_4 allows one-pot output and dramatically boosts photoredox catalytic activity, *Appl. Catal. B*, 2021, **295**, 120272.

S11 T. Huang, J. Chen, L. Zhang, Precursor-modified strategy to synthesize thin porous amino-rich graphitic carbon nitride with enhanced photocatalytic degradation of RhB and hydrogen evolution performances. *Chinese J. Catal.*, 2022, **43**, 497-506.

S12 M. Ge, X. Li, Z. Liu, M. Zhang, Enhanced photocatalytic degradation performance of cyano groups-modified carbon nitride nanosheets synthesized by magadiite template-assisted thermal treatment. *Mater Sci Semicond Process*, 2022, **141**, 106420.

S13 Q. Fan, J. Liu, Y. Yu, A simple fabrication for sulfur doped graphitic carbon nitride porous rods with excellent photocatalytic activity degrading RhB dye. *Appl. Surf. Sci.*, 2017, **391**, 360-368.

S14 G. Liu, M. Liao, Z. Zhang, Enhanced photodegradation performance of Rhodamine B with g-C_3N_4 modified by carbon nanotubes. *Sep. Purif. Technol.*, 2020, **244**, 116618.

S15 H. Xu, Y. Chang, X. Shen, Construction of Ag/AgCl-CN heterojunctions with enhanced photocatalytic activities for degrading contaminants in wastewater. *J. Colloid Interface Sci.*, 2019, **543**, 25-33.

S16 Y. Yang, H. Jin, C. Zhang, Nitrogen-deficient modified P-Cl co-doped graphitic carbon nitride with enhanced photocatalytic performance. *J. Alloys Compd.*, 2020, **821**, 153439.